

Precision Sampling Measurements using AC Programmable Josephson Voltage Standards

A. Rüfenacht, C.J. Burroughs, and S.P. Benz

National Institute of Standards and Technology, Boulder, CO 80305, USA

(Dated: November 20, 2007)

Abstract

We have performed a variety of precision measurements by comparing ac and dc waveforms generated by two independent ac programmable Josephson voltage standard (ACPJVS) systems. The objective of these experiments was to demonstrate the effectiveness of using a sampling digital voltmeter to measure small differences between Josephson waveforms. The low uncertainties that we obtained confirm the feasibility of using this sampling method for high accuracy comparisons between ACPJVS waveforms and signals from other sources. ¹

PACS numbers: 85.25.Cp

¹ Contribution of the U.S. government, not subject to copyright

I. INTRODUCTION

In order to increase the precision of primary standards for the ac electrical metrology community, the field of ac Josephson devices and systems has been steadily developing for more than a decade. The most accurate ac Josephson voltage standard (ACJVS) utilizes oversampled single-bit pulse-drive technology to achieve unprecedented low distortion and intrinsically accurate ac voltages [1, 2]. Unfortunately, the ACJVS output voltage is presently limited to 250 mV (rms). To generate higher dc and ac amplitudes of several volts, a multibit digital-to-analog converter based on staircase-approximated waveforms was developed by use of programmable Josephson voltage standards (PJVS) [3, 4]. When used as a precision ac voltage source, this ACPJVS system is capable of synthesizing waveforms that are ideally suited for applications at relatively low frequency such as electrical power metrology (50-60 Hz) [5–7].

Direct measurement of the rms voltage from ACPJVS waveforms reveals significant uncertainty contributions due to the transitions between the quantized Josephson voltage levels [8]. For high accuracy applications, this stepwise approximated method is limited to very low frequency waveforms until a more complete understanding of the transitions allows the output voltage to be precisely modeled so that correction factors can be applied. Because of these transient issues, we have decided to investigate sampling instead of rms measurement techniques for the new electrical power standard that is under development at NIST [6].

In order to avoid the large uncertainties associated with the above described transients in ACPJVS systems, both direct [9] and differential sampling techniques [10] have been proposed for ac power applications. In this case, only the sampled measurements where the voltage has fully settled into the quantized Josephson states are used [3], and all the samples that contain the transitions are discarded [8]. At NIST we are implementing a differential sampling approach to ac power measurements where we sample the voltage difference between a Josephson waveform and a separate sine wave of high spectral purity and stability. Using the differential method, we believe that the uncertainty of the sampling measurements can be significantly reduced since the sampling voltmeter is used as a null detector.

As a first step toward developing this differential sampling method, we present in this paper both directly sampled and differential measurements of ac waveforms synthesized by two independent ACPJVS systems. By comparing measurements of waveforms from two dif-

ferent ACPJVS systems, we determine the accuracy and uncertainty that are possible with the sampling method, as well as the noise characteristics of the sampling digital voltmeter (DVM). This paper extends the results published by Behr et al. [10] on the ac quantum voltmeter by using waveforms with more than four samples and with an enhanced uncertainty analysis. The gain and the linearity of the sampling DVM are measured at various frequencies using the differential method for lower voltages and by use of direct sampling for the higher voltages synthesized with a single ACPJVS system.

II. SAMPLING METHOD

Comparison measurements of two independent ACPJVS systems were performed using the configuration shown in Fig. 1. Each system contains current bias sources (DAC), a microwave frequency generator (CW), a microwave amplifier (AMP), and a PJVS superconducting integrated circuit. We used flex mounted PJVS chips [11] that can produce two different peak output voltages, 2.6 V and 3.9 V, each having the ternary programmable JVS design using SNS (superconductor - normal metal - superconductor) Josephson junctions arrays [12]. Other details of the Josephson circuits and systems have been described elsewhere [13]. For each system, the maximum output voltage is plus or minus 1.5 V rms, due to the output voltage limitation of the bias sources. Each generated voltage level V_j is selected by biasing a chosen number of Josephson junctions M_j . The proportional relation between these two quantities is given by $V_j = M_j f / K_{J-90}$, where f is the microwave bias frequency (18 GHz) and K_{J-90} is the Josephson constant (483 597.9 GHz/V). The two ACPJVS systems (A and B) are connected in a differential configuration (A-B) to the sampler (Agilent 3458A¹) that measures the voltage difference between the two waveforms (Fig. 1). The outputs of the two DAC units are floating and isolated from system grounds. To avoid any ground loops, the clock input and the trigger output signals of the DAC units are optically isolated. The galvanic isolation between the chip and the microwave amplifier is achieved with dc blocks (not shown).

¹ The commercial instruments are identified in this paper only in order to adequately specify the experimental procedure. Such identification does not imply recommendation or endorsement by the National Institute of Standards and Technology, nor does it imply that the equipment identified is necessarily the best available for the purpose.

We customized the sampling DVM so it could be locked to an external frequency reference. All the generated clock input signals are locked to the same 10 MHz reference. The fundamental frequency and number of samples used for each staircase-approximated waveform are identical for both ACPJVS systems. The output waveform amplitude of each system is independently adjustable, but generally chosen to be the same for each system in order to take advantage of the null detector configuration.

Synchronization of the two output waveforms is achieved by first loading both waveforms in the memories of the DAC units, followed by simultaneously turning on the clock reference signal to each system. We sample the waveform at twice its number of steps so that, for any sampling measurement, we keep only half of the points, namely those free of voltage transients, as shown in Fig. 2. Before each measurement sequence we carefully align the sampling window in the center of each step. This alignment is achieved by introducing a defined timing delay between the trigger input pulse and the start of the sampling procedure. The aperture (integration) time of the voltmeter is determined by the waveform frequency and twice the number of samples of the waveform. Since the sampler is a time domain instrument rather than a frequency domain instrument, the measured voltages contain dc thermal voltage offsets. To remove this undesired contribution for each voltage, we measured the waveform at both polarities using a positive-negative-negative-positive sequence ("+-+"). The negative polarity is selected by adding half the waveform period to the trigger delay. This sequence is then repeated many times to obtain sufficient statistics for the computation of the mean value and the associated uncertainty for each of the steps.

III. DIFFERENCE MEASUREMENTS (2.6V - 2.6V)

In order to demonstrate precise agreement between two ACPJVS systems, this section is dedicated to sampled comparisons of identical waveforms from two identical 2.6 V chips. In this configuration, every voltage step in the waveform uses exactly the same number of active junctions for both chips. If the two microwave bias frequencies are also identical, the resulting differential signal should be precisely zero (excluding samples occurring during transitions) and should reflect only the noise floor of the experiment. By introducing a small difference between these two microwave frequencies, we can generate a differential waveform of the same shape as the two original ones, but with any desired small difference

amplitude between 0 and 1.5 mV (peak). This procedure allows us to check the ability of the DVM in the sampling mode to accurately resolve voltages different from zero at various waveform frequencies. Additionally, the small voltage levels generated can be used to test the gain error of the voltmeter in this differential configuration. This topic will be discussed further toward the end of this paper. For this comparison, the amplitude of the stepwise-approximated sine wave waveform A is fixed at the nominal calculated value of 1 V rms. The chosen amplitudes for waveform B are slightly higher than 1 V rms in order to generate the desired small, difference voltages (A-B) of 10 μ V, 100 μ V, and 1 μ V (peak voltage). The differential signals at each of these three amplitudes were measured for the cases containing 4, 32 and 64 samples. Finally, we tested all of these waveform configurations at various frequencies, from 0.3 Hz (64 samples) to 3.6 kHz (4 samples). The data presented in the following figures correspond to the mean value of 500 measured points, where the offset has been removed using the "+--+" sampling sequence described in the previous section. The error bars represent the standard deviation of the mean with $k=2$, corresponding to a confidence interval of 95 %. Figure 3 presents an overview of the sampling measurement results for the voltages from steps 43 through 51 for waveforms with different frequencies containing 64 samples and with peak differential voltage amplitudes of 10 μ V. The inset represents the expected differential voltage steps for the full period of the same waveform. For clarity, the number of frequencies shown here has been limited to five (0.3, 3, 15, 60 and 150 Hz). As explained before, only half of the measured sampling points are presented, since the samples containing the transients are discarded. Figure 4(a) shows the same measurement data (steps 43 through 51), but plotted in terms of the voltage difference from the expected ideal waveform step. For comparison, Fig. 4 also presents data from the 100 μ V and 1 mV amplitude differential waveforms. All these data were acquired on the 100 mV range of the sampler, and one key feature of the results is that the magnitude of the standard deviation of the mean at each step does not depend on the amplitude of the waveform. All three sets of data exhibit the same uncertainty for a given waveform frequency.

All of the measurement points within the uncertainty bars ($k=2$) are close to the expected Josephson step reference voltages. However, some significant deviations appear for the highest waveform frequencies (150 Hz). In order to elucidate this effect, we analyzed the uncertainties of our measurements using two distinct quantities. The first quantity, called σ_{noise} , is the standard deviation of the mean represented by the error bars on Figs.

3 and 4, and derived from statistical calculations of the 500 measured points. The second quantity, σ_{dev} , is related to the standard deviation of the difference of the mean measured step voltage from its expected Josephson voltage for the sampled steps in the waveform at a given frequency. In this particular case, we assume that both Josephson systems are working perfectly. For particular frequencies, σ_{dev} can be larger than the type A uncertainty noise, as observed for the data at 150 Hz on figures 3 and 4. Note that the largest peak amplitude, (1 mV) corresponds to only 1 % of the selected voltmeter range (100 mV), which is the scenario where the sampling voltmeter is assumed to operate as a null detector.

A. Type A uncertainty (σ_{noise})

Figure 5 shows the results of the type A uncertainty (σ_{noise} , standard deviation of the mean, $k=2$) as a function of waveform frequency for three different waveform shapes (4, 32 and 64 samples) [10]. The uncertainty reported is the average of the individual contributions from all the steps. As we increase the number of steps in the waveform, the time window used by the sampler to measure the voltage signal decreases. Since the measurement uncertainty depends principally on this voltmeter aperture time, the data with more samples show a larger uncertainty for a given waveform frequency because the aperture time is smaller for each sample. At 60 Hz, the frequency of electric power applications, the standard deviation of the mean is less than 85 nV, 56 nV and 21 nV, respectively, for the 64, 32 and 4 sample waveforms. For the 64 sample waveform, the value corresponds to an uncertainty of 6 parts in 10^8 (reference 1.41 V, full waveform peak amplitude). At frequencies lower than 10 Hz, this value is less than 30 nV (corresponding to 2.2 parts in 10^8) for all the waveforms reported here. The sampling technique gives better performance for lower frequency waveforms and smaller numbers of samples.

The aperture time of the voltmeter (τ) is defined as $\tau = (2Nf)^{-1} - \delta t$, where N is the number of samples in the waveform, f is the frequency of the waveform, and δt the setup time of the sampling voltmeter. The factor 2 in this expression arises because the sampling is performed at twice the number of steps in the waveform to reject the transient contributions. The value of δt depends on the type of sampling DVM, and for the Agilent 3458A it is fixed at 30 μs . If we plot the uncertainty in terms of the aperture time of the voltmeter instead

of the waveform frequency, we observe a scaling behavior between all the measurements, as shown in Fig. 6. The slope of the data trend gives an exponent of -0.48, close to the expected value -1/2. The uncertainty measured is practically independent of both the amplitude of the differential waveform and the number of samples. At low aperture times, we observe a varying and higher uncertainty for the four sample waveform. This inconsistency is possibly due to some other effect concerning the triggering and timing at higher frequencies (up to 3.6 kHz for the waveforms containing only four steps). The noise level of the voltmeter in the sampling mode is of the order of $1 \text{ nV}/\sqrt{\text{Hz}}$, where the frequency bandwidth is determined by the inverse aperture time $\sigma_{noise}(\text{V}) = 10^{-9} \cdot \tau(\text{s})^{-1/2}$. These scaling parameters extracted from Fig. 6 determine the operation margins (noise level) of the present sampling method. For instance, if we would like the type A uncertainty ($k=2$) to remain below $0.1 \text{ } \mu\text{V}$ at 60 Hz, we may choose at most 80 steps in the waveform. These measurements also reveal the limitations of the sampling technique for waveforms at high frequencies and high numbers of samples.

B. Deviation from ideal Josephson value (σ_{dev})

For each waveform, σ_{dev} represents the standard deviation calculated from the set $\{\Delta V_i\}$ containing all the individual voltage differences. For a given voltage step i , ΔV_i is defined as the voltage difference between the mean measured voltage and the corresponding Josephson voltage difference between the two arrays. Figure 7 shows the dependence of σ_{dev} as a function of the aperture time τ . The data presented here are derived from waveforms with amplitude of 1 mV (zero to peak). The standard deviation ($k=2$) reported in this figure represents a confidence interval of 95 % and gives a good estimate of the largest deviation expected for an individual step. The scatter of the points in this logarithm-logarithm plot (Fig. 7) is particularly large in comparison with the tight scaling trend of the Type A uncertainty shown in Fig. 6. Nevertheless, a general tendency, represented by the solid line, is observed. The standard deviation of the voltage difference can be linked to the aperture time of the voltmeter with the following relation ($k=2$): $\sigma_{dev}(\text{V}) \approx 2 \cdot 10^{-9} \cdot (\tau(\text{s})^{-1/2} - 1)$. Using this relation, the largest deviation from any Josephson step of a waveform (60 Hz, 64 samples) is smaller than $0.2 \text{ } \mu\text{V}$. This rather pessimistic ($k=2$) approach gives an upper limit for the accuracy limitation. Nevertheless, since these deviations are

scattered equally about zero, their impact on the rms calculation of the waveform are much less significant (see section IV). From these data, we note that both accuracy (σ_{dev}) and noise level (σ_{noise}) are linked with the inverted square root of the aperture time. We conclude that these two uncertainty mechanisms (σ_{dev} and σ_{noise}) are dominated by effects involving only the sampling voltmeter. Therefore, both ACPJVS systems behave as expected as quantum accurate references. Comparison between two precision reference sources provides an interesting measurement technique to characterize the behavior of the sampler² in the limit of low input voltages.

IV. DIFFERENCE MEASUREMENTS (2.6V - 3.9V)

The advantage of the sampling method with twice the number of samples is that the samples having transient contributions can be removed. By using the measured amplitude of the constant step $\{V_i\}$, we can reconstruct the rms voltage of the full waveform. By selecting one of the two ACPJVS systems as reference $\{J_i\}$ we can reconstruct the rms value (V_{rms}) of the other system by measuring the voltage differences $\{M_i\}$ for all the different steps $i = 1 \dots N$ using the following relation (Eq. 1):

$$V_{rms}^2 = \frac{1}{N} \sum_{i=1}^N V_i^2 = \sum_{i=1}^N (J_i + M_i)^2. \quad (1)$$

This pseudo-rms or reconstructed rms calculated quantity should not be confused with the rms value of the full staircase-approximated output waveform, which contains contributions from the transients. However, it can be useful to compare this reconstructed rms voltage with the ideal rms voltage (that assumes zero rise time between output levels), which is easily calculated from the known quantized Josephson voltages. In the various plots of this section, we report the voltage difference between those two quantities. The uncertainty associated with the rms value ($\sigma_{V_{rms}}$) is derived from the type A uncertainties σ_{M_i} , measured for each voltage step (Eq. 2):

$$\sigma_{V_{rms}} = \frac{\sqrt{\frac{1}{N} \sum_{i=1}^N (2M_i + 2J_i)^2 \cdot \sigma_{M_i}^2}}{2 \cdot \sqrt{\frac{1}{N} \sum_{i=1}^N (M_i + J_i)^2}}. \quad (2)$$

² Manufacturer description of sampling technique and Analog-to-Digital Converter used inside the Agilent 3458A [14].

Any deviation of the reconstructed rms voltage from the ideal rms voltage indicates that one or both of the waveforms are not within operation margins, or that there is poor time alignment between the waveform and the sampling voltmeter. The systematic errors associated with σ_{dev} (in previous section) have essentially no rms contribution and thus do not strongly affect $\sigma_{V_{rms}}$. In this section we present two different tests of the operating margins that are necessary to ensure that both systems generate precisely quantized voltages. In order to produce small but finite differential voltages M_i at each sample, we chose PJVS chips with different numbers of junctions for each step, namely a 2.6 V chip and a 3.9 V chip. The resulting differential voltage waveform is no longer sinusoidal, as were the waveforms used in the previous section. The differential waveform is not sinusoidal because the number of junctions and the combination of cells utilized to produce any voltage step of the waveform are different for the two chips, even if both circuits produce the same desired rms voltage. For example, the smallest cell in each array is 16 junctions for the 2.6 V chip and 24 junctions for the 3.9 V chip.

When both microwave bias frequencies are identical, the expected difference waveform will correspond to an integer number of Josephson junctions. For equal microwave frequencies, the first quantized voltage corresponds to a voltage difference of two junctions ($74.4 \mu\text{V}$ at the 18 GHz bias frequency). For the experiment described below, the microwave frequencies are not identical in order to exactly match the rms output voltage (1.5 V rms). In this case deviations from each quantized level are observed, as shown in Fig. 8. The pattern depends only on the amplitude and the number of samples of the two generated waveforms. Note that the pattern is completely symmetric in sample number, a condition required for the offset subtraction method. The patterns shown in Fig. 8 produce an interesting waveform with voltages that are different from zero and within the null-detection (lowest) range of the sampler. The maximum peak amplitude is around $400 \mu\text{V}$. Similar waveforms are planned for future comparisons between the ACPJVS system and a stable sine wave of high spectral purity.

A. Time alignment between the two synthesized waveforms and the sampling DVM

Before any comparison measurement can be performed, the synthesized waveforms must be time aligned with the sampling window of the voltmeter. The delay between the trigger pulse from the DAC electronics and the beginning of the sampling sequence is adjusted to obtain samples that are centered in the middle of the Josephson steps. To determine the effect of misalignment, measurements were performed for different time delays so that the resulting reconstructed rms voltages could be compared. As we explored this effect for different frequencies, the delay value was rescaled in terms of the percentage of the sampling time duration. Since the sampling duration corresponds to half of the Josephson step length, we expect to observe a constant voltage region or "flat spot" for delays between $\pm 50\%$ of the sample duration where the voltages of both Josephson arrays are fully settled. For the two extreme values (at -50% and $+50\%$), a corner of the sampling window is aligned respectively with either the beginning or ending edge of the Josephson step. If this limit is exceeded, the reconstructed rms voltage will contain contributions due to the transients. Figure 9 shows the voltage difference between the reconstructed rms voltage and the expected ideal rms voltage of array B for waveform frequencies of 60 Hz and 300 Hz. The uncertainty reported corresponds to the standard deviation of the mean ($k=2$), determined from 50 measurements.

Over a time shift of 48 %, the data at 60 Hz show no significant deviations. At 300 Hz, the sampling time margins are slightly reduced (-40% to 45%). Around -50% the bump in the data reflects the presence of residual ringing for each Josephson level. This effect starts to appear when the waveform frequency increases. As discussed before, the uncertainty is larger for the higher frequency waveform. Nevertheless, both waveforms show a large flat spot, such that a small deviation in the time alignment around the center of the step doesn't affect the accuracy of the measurement of the reconstructed rms voltage. Note that this same alignment procedure will be needed in future measurements when we compare a sine wave of high spectral purity with a staircase-approximated ACPJVS sine wave.

B. Operating margins and dither-current flat spot

To be a useful system, the ACPJVS must generate an accurate voltage over a range of bias parameters. The most critical bias parameter for the ACPJVS system is the current margin or step width; that is, it must produce an accurate voltage over a large range of dc current through the entire multiple-array circuit. For dc voltages, a nanovoltmeter is used to determine the array's immunity to an applied dither current [13]. To determine the operating margins for a sampled synthesized ac waveform requires a measurement instrument that can resolve a few microvolts on a 1 V rms scale. The sampler can provide a fast, direct measurement of the full-waveform rms amplitude, but the uncertainty obtained in this case is not as good as the uncertainty achieved when measuring dc voltages because it includes errors from the transients and voltage nonlinearities of the sampler. Nevertheless, a more precise analysis can be performed by using differential sampling (with different arrays, such as 3.9 V and 2.6 V chips) and determining the rms amplitude from the reconstructed stepwise-approximated sine wave that was sampled on constant voltage steps. The operating margins of array B can be determined by applying a dither current to array B, while using voltage steps of array A as reference levels. Figure 10 presents the measured differences between the reconstructed and the ideal rms voltages for 60 Hz waveforms at 32 and 64 samples (uncertainty $k=2$, for a set of 50 measured points). The flat spots of the reconstructed rms voltages show a constant voltage over a current range of at least 1.5 mA. Even if the cell combinations are different for the two waveforms, the measured current margins are similar, as expected.

The current range over which the reconstructed rms voltage remains constant is a direct measure of the immunity of the weakest cell in array B to an applied dither current. The flat spot is centered on -0.25 mA (which would ideally be zero), and the source of this shift is certainly related to two different additive effects:

(i) A voltage step is achieved by a combination of the different cells, where each bias current is defined individually. Small deviations from the expected ideal bias current may appear in this particular configuration [8]. This effect is probably enhanced when an ac-waveform is generated containing a rapid succession of different cell combinations.

(ii) Since these measurements are performed using the differential configuration with two separate systems, some unexpected current may also come from interaction of the two DAC

bias sources or from grounding issues (although we would expect these error mechanisms to be more of an issue above audio frequencies, and relatively small at 60 Hz). In either case, these results show the importance of characterizing the ACPJVS operating margins and ensuring that they are sufficiently large.

C. Accuracy of the difference measurements

In previous sections we explored the measurement uncertainty of individual samples and the bias current and sampling time margins of the ACPJVS measurement system. In this section we determine the voltage accuracy and uncertainty of the sampled rms waveforms in the differential measurement configuration as a function of frequency. As in the previous section, we use two arrays with two different waveforms and reconstruct the rms voltage of one array utilizing the voltage steps of the other array as a reference. We discard the samples containing the transients and compute the ideal rms voltage of the stepwise portions of the synthesized waveforms.

Figure 11 shows the voltage difference between the ideal and reconstructed measured waveform for 32 and 64 samples at various frequencies (array B, 2.6 V chip). The plotted uncertainty corresponds to the standard deviation of the mean ($k=2$) with 500 measured points. This uncertainty is calculated with the type A uncertainty associated with each voltage level (Eq. 2). We emphasize that all the measured points up to 60 Hz are within 15 nV of the ideal rms value. As the full amplitude of both waveforms is 1.5 V rms, the relative accuracy of the reconstructed rms voltage is better than 10 nV/V (up to 64 samples per waveform). This result is a striking demonstration of the excellent agreement between the two ACPJVS systems. As expected, the uncertainty increases as the aperture time of the voltmeter decreases. Nevertheless, for a given aperture time, the deviation from the ideal rms value is much smaller than σ_{dev} described in the previous section. This effect is due to the averaging of the σ_{dev} uncertainties in the calculation of the rms value. However, the impressive accuracy achieved with the sampling voltmeter at 60 Hz is certainly suitable for power metrology applications.

V. DVM GAIN AND LINEARITY ANALYSIS

Knowledge of the gain correction and linearity of an instrument is an important factor in the determination of uncertainty budgets. Presently, programmable and conventional Josephson systems are widely used for calibrating the gain of dc voltmeters. The sampling method (using one ACPJVS or two ACPJVS systems differentially) allows us to test DVM gain correction factors in both dc and sampling modes.

A. Measurements of dc gain

First we measured the gain characteristics of the DVM in dc mode. All the measurements presented here were performed on the 100 mV range since we are primarily interested in small amplitude voltages. The smallest step voltage from the PJVS is achieved by biasing 16 junctions at a microwave frequency of 18 GHz (2.6 V chip) which produces a dc voltage of $596\text{ }\mu\text{V}$. All achievable voltages are quantized and correspond to a multiple of this least significant bit (LSB) voltage. Only three quantized voltages, both polarities of this LSB voltage and zero, can be reached within a span of 1 mV. At higher voltages, when a large number of Josephson junctions is used, sub-microvolt resolution can be achieved by changing the microwave frequency. In this situation, the resolution of the output voltage is dictated by the frequency resolution of the microwave source. By using two programmable arrays in a differentially coupled configuration (two 2.6 V chips), we can achieve high resolution even for small voltages by biasing each array at a large voltage (large number of junctions) with slightly different microwave bias frequencies. Calibration of the low voltage ranges of digital voltmeters (1 and 10 mV) is a promising application for this technique. An interesting application of this technique is to use two such PJVS systems (or arrays) as a "quantum null detector" by differentially coupling an unknown low voltage source and a low voltage Josephson reference with a nanovoltmeter.

Figure 12 presents measured data in dc mode of the voltmeter gain on its 100 mV range. Careful offset (that is thermal voltage) subtraction has been performed by measuring the "0" voltage step between every pair of voltage polarities. The offset voltage (and first order drift in time) is removed for both polarities, and the voltage pairs are measured in random order. This measurement sequence is repeated three times, and the uncertainty plotted corresponds

to the standard deviation ($k=1$) of each voltage measurement. The quantity on the Y axis is the difference between the measured step voltage and the Josephson quantized voltage. Figure 12(a) presents, over the 1 mV voltage range, the measured gain of the voltmeter by use of the differential method with two 2.6 V chips. There is no noticeable gain nonlinearity for this amplitude range near zero. The calculated slope gives a deviation of 0.54 V/V, corresponding to an error of only 0.5 nV at 1 mV, a value 100 times smaller than the measured noise floor. Assuming that this gain error is insignificant, a statistical analysis of the measured data provides a determination of the voltmeter's noise floor near zero voltage. The two opposite horizontal dashed lines (± 48 nV) show the standard deviation ($k=2$) of all the measured points in Fig. 12(a). For comparison, Fig. 12(b) shows the gain of the same voltmeter over the full scale of its 100 mV range. In this case, the reference voltage levels are generated with a single Josephson system. We observe a gain error of $-4.44 \mu\text{V/V}$ with excellent linearity, and a maximum deviation from the straight-line fit of 60 nV.

B. Gain in the sampling mode

To measure the gain performance of the voltmeter in the sampling mode, we used triangular waveforms containing 32 samples at various frequencies. Each step of the waveform was compared with the expected Josephson reference voltage. Since the triangular waveform was symmetric, each voltage level was measured twice, once each while the voltage is ascending and descending. Just as in the DC gain measurements discussed above, for the sampling mode linearity measurements we similarly investigated the 1 mV and 100 mV waveform amplitudes. To obtain the 1 mV amplitude triangular waveform, we used the same differential technique (two 2.6 V chips) explained in detail in section III. Likewise for the dc measurements, the 100 mV amplitude waveforms were directly generated with a single ACPJVS system. Figure 13 presents the voltage difference of the measured and ideal Josephson voltage steps as function of the step amplitude, for the different frequencies 0.6 Hz, 60 Hz and 200 Hz. As in the dc linearity measurements, we observe no gain deviation for the 1 mV amplitude waveforms shown in Fig. 13(a). The uncertainty (standard deviation of the mean for 500 measurements, $k=2$) increases with the frequency, which exactly follows the expected dependence on the aperture time that was discussed in section III. The voltage accuracy, that is, the scattering of the voltage differences around zero, is also related to the

aperture time (reflecting the presence of dev discussed in section III). Note that the offset subtraction technique is not perfect. For example, the 0.6 Hz data set presents a remaining offset of -13 nV. Other measurements performed with lower amplitude (100 μ V and 10 μ V) sine wave waveforms, lead to the same conclusions. For measurements over the full 100 mV voltage range (Fig. 13(b)), we observe an interesting behavior that is much different from the dc linearity measurements. In the limit of large aperture time, the voltmeter in the sampling mode behaves as in the DC mode. For a frequency of 0.6 Hz, the measured differences are linear and a gain error can be easily extracted. However, this -0.42 V/V value is slightly different than the one measured in the DC case (see Fig. 12(b)). This difference may be attributed to the variation of the gain with external conditions, such as temperature, because the measurements were performed on different days. However, as the aperture time decreased, the measured gain error increased, including a sign change of the slope. For example, the gain factor at 60 Hz is +4.4 V/V and the largest deviation from the calculated gain is about 0.44 μ V. For higher frequencies (and smaller aperture times), the gain error becomes more nonlinear with higher uncertainty.

This behavior changes dramatically when the aperture time is below $\sim 100 \mu$ s. In this case, meaningful evaluation of gain and linearity cannot be accomplished because the non-linearity effects are extremely large and the sampled waveform becomes history dependent. These data at 200 Hz and 100 mV particularly illustrate this behavior, which appears hysteric. The largest deviation observed in Fig. 12(b) is 1.3 μ V. The cause of this large history-dependent nonlinearity is unknown and can be accounted for only by attributing a very large Type A uncertainty to these measurements. For the sampled data with higher aperture time (for instance 60 Hz with 32 samples), we also require larger uncertainties to account for the observed nonlinearity effects, which are much greater than those found for the dc linearity measurements. To balance this rather pessimistic analysis of the sampled waveform linearity results, one should keep in mind that such measurements are once again testing the limits of the sampling voltmeter's capabilities, which are already outstanding. Nevertheless, when the sampler is used properly with sufficient aperture time, the linearity and uncertainty results suggest that the sampling DVM can be successfully used with the differential measurement technique for applications at 60 Hz with sufficient voltage resolution. In this configuration, no particular gain and linearity corrections need to be applied, provided that the amplitude differences between the high spectral purity sine wave and the

Josephson stepwise-approximated waveform remain below a few millivolts, which is a small fraction of the sampling DVM's lowest voltage range.

VI. CONCLUSION

The results in this paper demonstrate that sampling small differences between two waveforms allows us to achieve much lower uncertainties than are possible when sampling the full range of directly synthesized waveforms. Synchronized sampling is essential for achieving the lowest uncertainty, because samples occurring during ACPJVS transitions can be discarded so that comparisons can be based entirely upon the fully settled, perfectly quantized, Josephson voltage steps. We found excellent agreement between two ACPJVS systems of less than 1 part in 10^8 (reconstructed rms amplitude) when generating 64-state stepwise-approximated sine waves at 60 Hz. We also demonstrated the feasibility of using an ACPJVS waveform and measured difference data to determine the rms voltage of another waveform, not precisely known, but highly stable. We plan to implement the sampling techniques described in this paper in a new quantum-based system for calibrating 60 Hz voltage waveforms that should reduce the measurement uncertainty for calibrating power meters. Our results suggest that it is possible to achieve an uncertainty of a few parts in 10^7 for measurements of an independent reference sine wave of high spectral purity and stability. The number of samples chosen will be determined by balancing the increased uncertainty from nonlinearity effects that appear at small sample numbers due to larger voltage differences with the increased uncertainty for high numbers of samples that require short aperture times .

Acknowledgments

We thank Tom Nelson and Bryan Waltrip, NIST Gaithersburg, for advice regarding sampling techniques and customization of the DVM to implement the external clock reference. We are grateful to Paul Dresselhaus, Yonuk Chong, Nicolas Hadacek, Burm Baek, and Michio Watanabe for helping develop the stacked junction fabrication process used for our PJVS chips. We thank Jonathan Williams of NPL for helpful conversations and support regarding the bias electronics [15]. We also thank Ralf Behr and Luis Palafox of PTB for collaborative discussions regarding ac waveform synthesis using Josephson arrays. Rod White

suggested helpful approaches to elucidating the systematic deviations observed in the higher frequency differential measurements.

-
- [1] S.P. Benz and C.A. Hamilton, "Application of the Josephson effect to voltage metrology," Proc. of the IEEE, vol. **92**, 1617 (2004).
 - [2] S.P. Benz, C.J. Burroughs, P.D. Dresselhaus, N.F. Bergren, T.E. Lipe, J.R. Kinard, and Y.H. Tang, "An AC Josephson voltage standard for AC-DC transfer standard measurements," IEEE Trans. Instrum. Meas. **56**, 239 (2007).
 - [3] C.A. Hamilton, C.J. Burroughs, and R.L. Kautz, "Josephson D/A converter with fundamental accuracy," IEEE Trans. Instrum. Meas. **44**, 223(1995).
 - [4] R. Behr, J.M. Williams, P. Patel, T.J.B.M. Janssen, T. Funck, and M. Klonz, "Synthesis of precision waveforms using a SINIS Josephson junction array," IEEE Trans. Instrum. Meas. **54**, 612 (2005).
 - [5] R. Behr, L. Palafox, J. Schurr, J.M. Williams, and J. Welcher, "Quantum effects as a basis for impedance and power metrology," in Proc. of the 6th International Seminar in Electrical Metrology, pp. 11-12, Sep 21-23 2005, Rio de Janeiro, Brazil.
 - [6] C.J. Burroughs, S.P. Benz, P.D. Dresselhaus, B.C. Waltrip, T.L. Nelson, Y. Chong, J.M. Williams, D. Henderson, P. Patel, L. Palafox, and R. Behr, "Development of a 60 Hz power standard using SNS programmable Josephson voltage standards," IEEE Trans. Instrum. Meas. **56**, 289 (2007).
 - [7] L. Palafox, G. Ramm, R. Behr, W.G.K Ihlenfeld, and H. Moser, "Primary ac power standard based upon programmable Josephson junction arrays," IEEE Trans. Instrum. Meas. **56**, 534 (2007).
 - [8] C.J. Burroughs, A. Rufenacht, S.P. Benz, P.D. Dresselhaus, B.C. Waltrip, and T.L. Nelson "Error and Transient Analysis of Stepwise-Approximated Sinewaves Generated by Programmable Josephson Voltage Standards," in Proc. of the National Conference of Standards Laboratories International, Jul 30-Aug 2, 2007, St. Paul, Minnesota, and to appear in IEEE Trans. Instrum. Meas. April 2008.
 - [9] W. G. Krten Ihlenfeld, E. Mohns, R. Behr, J. M. Williams, G. Ramm and H. Bachmair, "Characterization of a high-resolution analog-to-digital converter with an AC Josephson source,"

- IEEE Trans. Instrum. Meas. **54**, 612 (2005).
- [10] R. Behr, L. Palafox, G. Ramm, H. Moser, and J. Melcher, "Direct comparison of Josephson waveforms using an ac quantum voltmeter," IEEE Trans. Instrum. Meas., **56**, 235 (2007).
 - [11] C.J. Burroughs, P.D. Dresselhaus, Y. Chong, and H. Yamamori, "Flexible Cryo-Packages for Josephson Devices," IEEE Trans. Appl. Supercon. **15**, 465 (2005).
 - [12] Y. Chong, C.J. Burroughs, P.D. Dresselhaus, N. Hadacek, H. Yamamori, and S.P. Benz, "Practical high resolution programmable Josephson voltage standards using double- and triple-stacked MoSi₂ barrier junctions," IEEE Trans. Appl. Supercon. **15**, 461 (2005).
 - [13] C.J. Burroughs, S.P. Benz, T.E. Harvey, and C.A. Hamilton, "1 Volt dc programmable Josephson voltage standard," IEEE Trans. Appl. Supercon. **9**, 4145 (1999).
 - [14] Hewlett-Packard JOURNAL, April 1989.
 - [15] P. Kleinschmidt, P.D. Patel, J.M. Williams, and T.J.B.M. Janssen, "Investigation of binary Josephson arrays for arbitrary waveform synthesis", IEEE Proc.-Sci. Meas. Technol. **149**, 313 (2002).

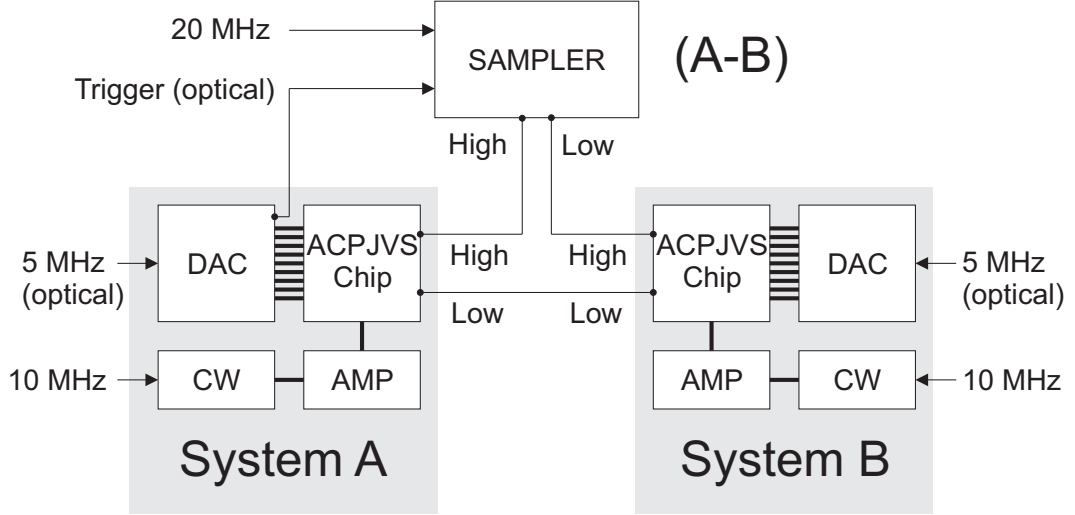


FIG. 1: Schematic of the differential sampling configuration used for comparing the voltages synthesized by two ACPJVS systems.

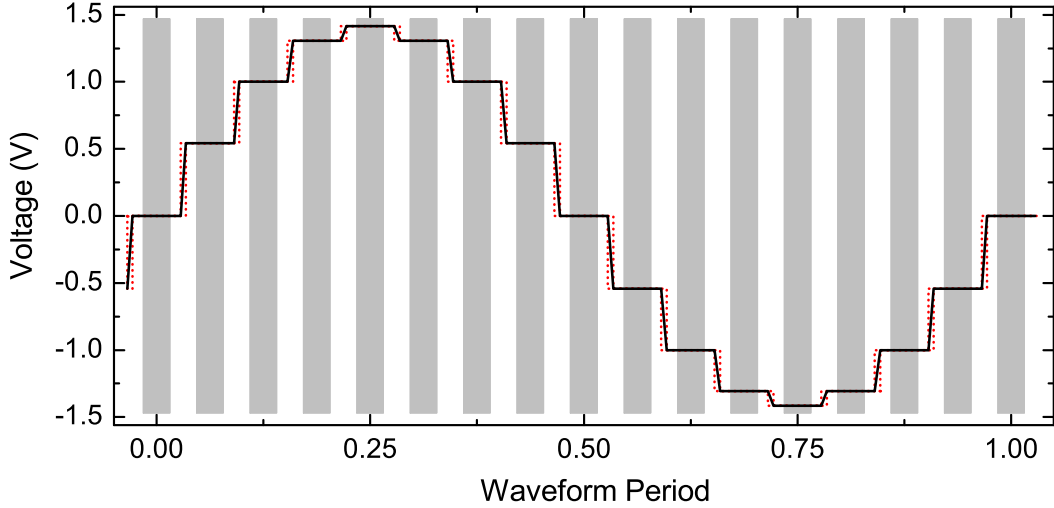


FIG. 2: Time-dependent voltage plot showing the sampling windows for a waveform containing 16 samples at an amplitude of 1 V rms. In this example waveform, alternating gray and white time slices represent different time integration windows of the sampling voltmeter. The gray zones are free of transients and therefore sample only the parts of the waveform where the voltage is accurately established. We discard the white sampling zones that contain the transients where the voltage is changing between steps.

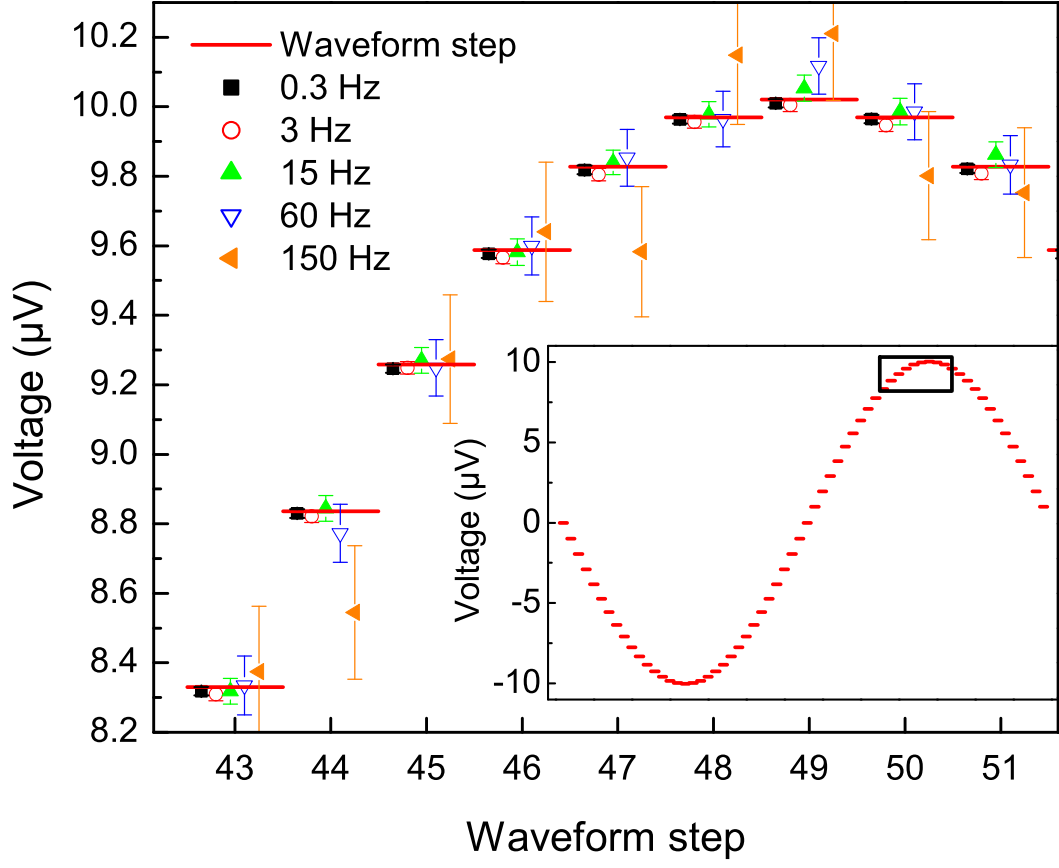


FIG. 3: (Color online) Sampled voltages from a differential waveform containing 64 steps with 10 μV peak amplitude for 5 different frequencies. The inset shows the stepwise voltages for a full waveform period and the rectangle illustrates the data range presented in the main frame, namely steps 43 through 51.

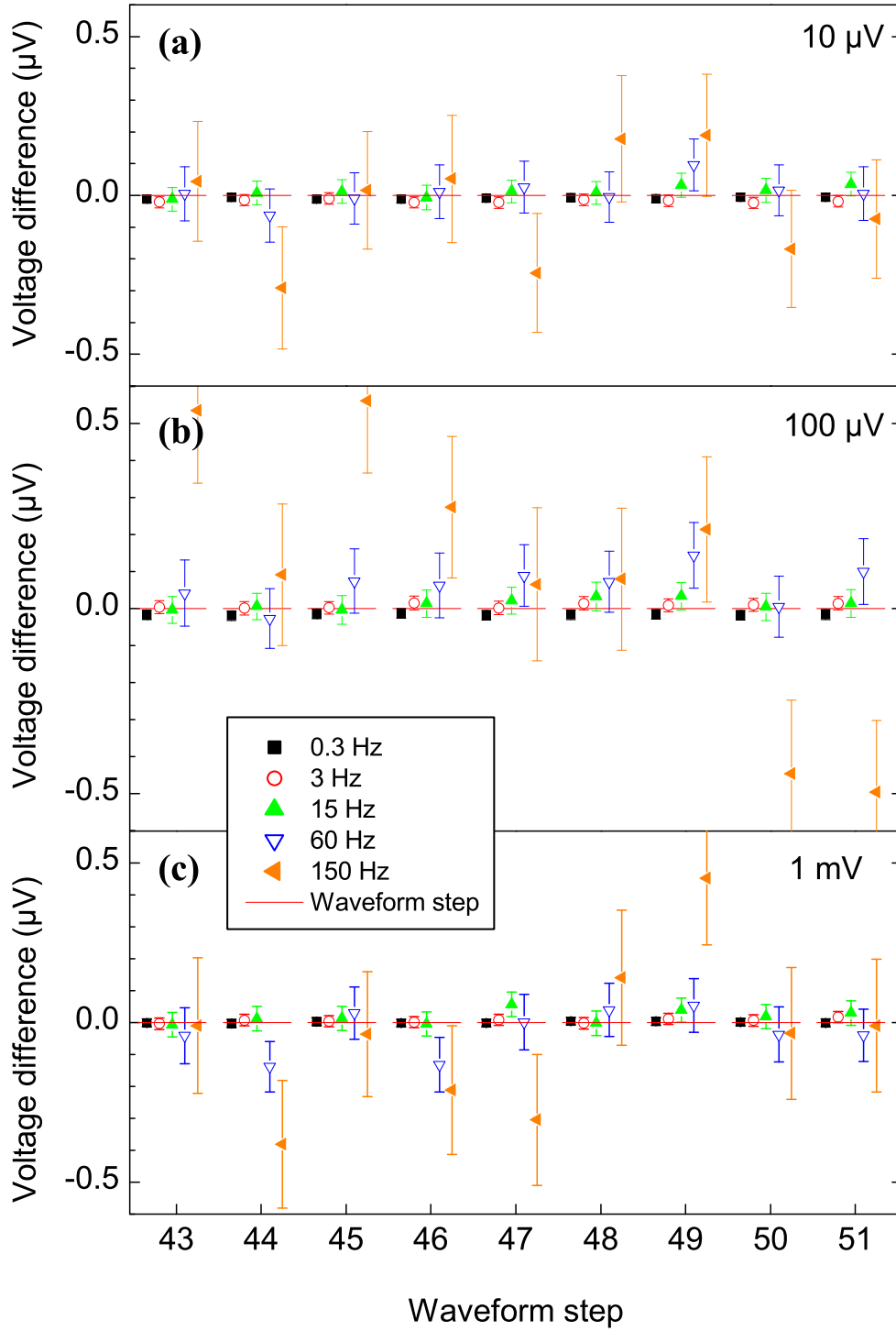


FIG. 4: (Color online) Difference between the expected Josephson voltage and the measured voltage, for 64 sample waveforms of different frequencies. Step numbers 43 to 51 are presented here. The uncertainties are clearly independent of the differential amplitude ($10 \mu\text{V}$, $100 \mu\text{V}$ and 1 mV) of the waveform and dependent on the waveform frequency. Thus the uncertainty depends primarily on the sampler's aperture time.

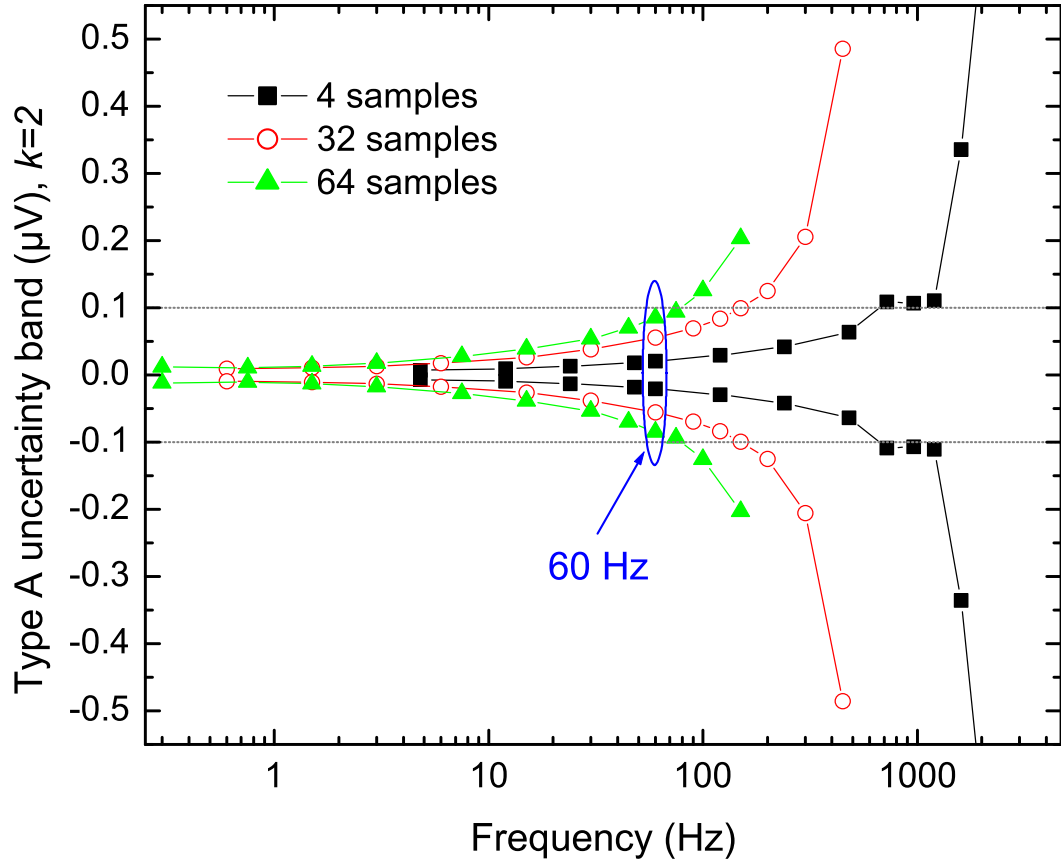


FIG. 5: (Color online) Type A uncertainty ($k=2$, averaged over the number of samples) measured for 1 mV amplitude waveforms with various sample numbers (4, 32 and 64) as a function of the waveform frequency.

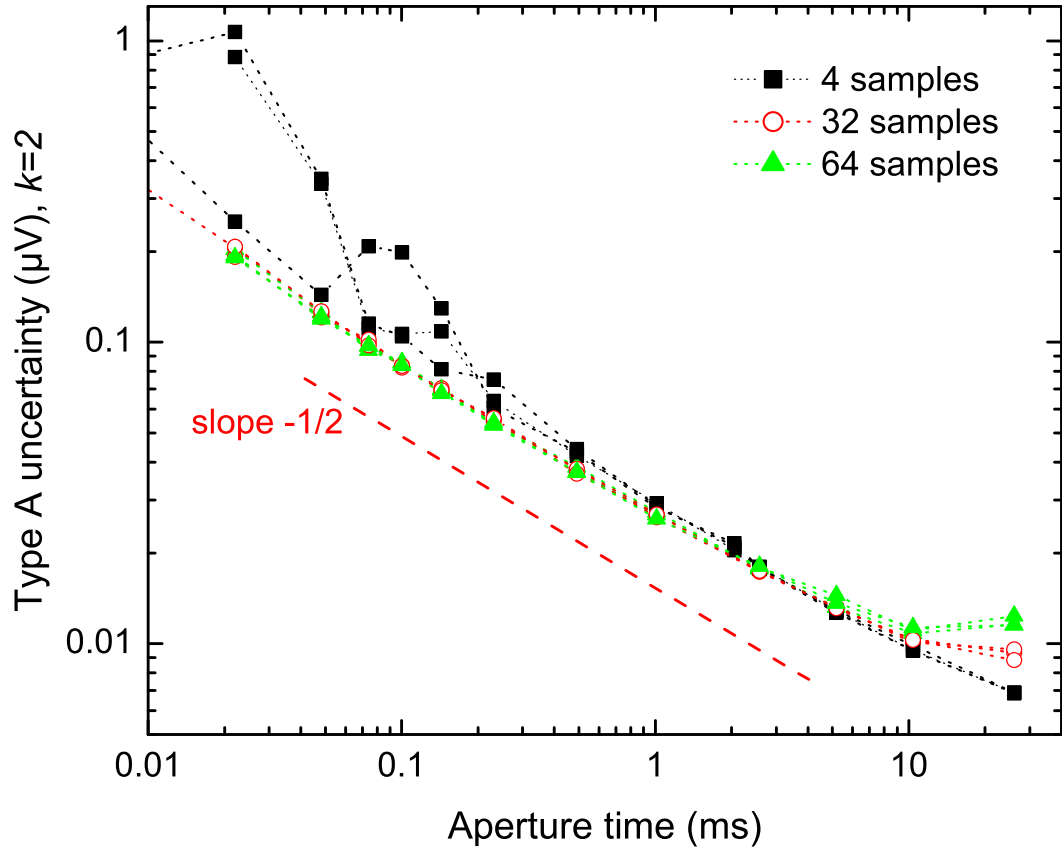


FIG. 6: (Color online) Measured Type A uncertainties (for 10 μV , 100 μV and 1 mV differential waveforms) as a function of the aperture time of the voltmeter. The dashed line shows slope -1/2 as a guide to the eye.

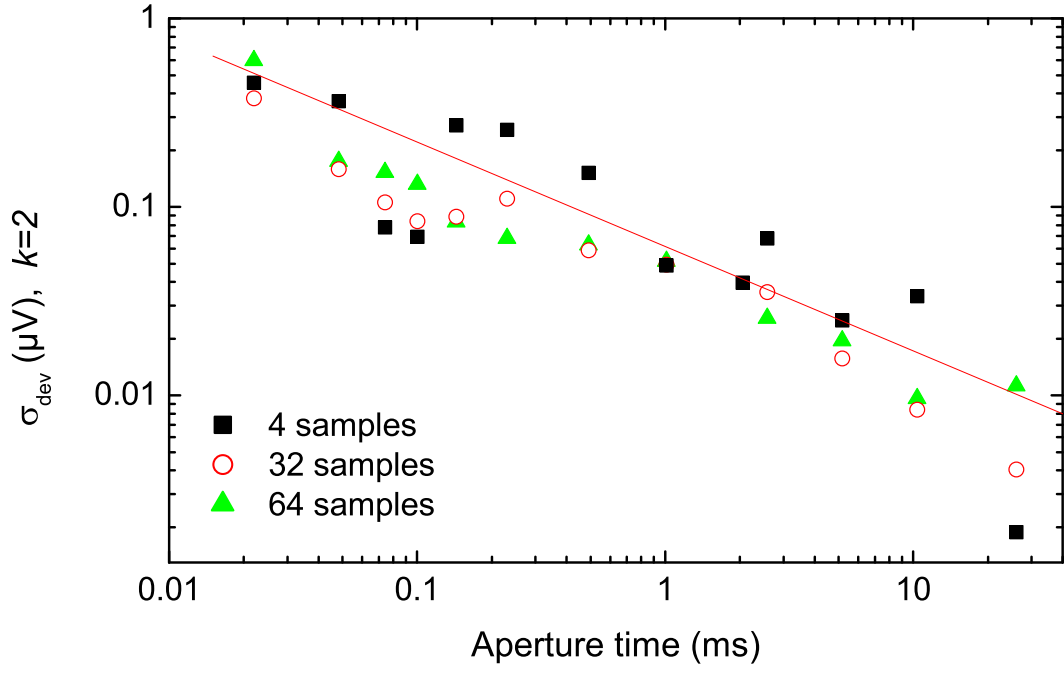


FIG. 7: (Color online) Standard deviation σ_{dev} (for 1 mV differential waveforms) as a function of the voltmeter aperture time. The line (slope -1/2) gives the general trend of the data dependence for this aperture time range.

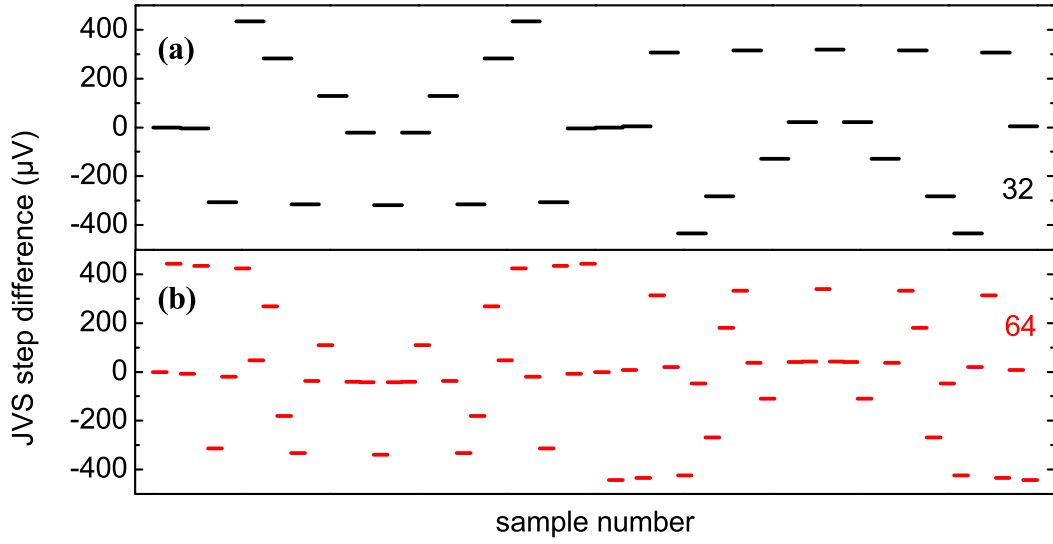


FIG. 8: (Color online) Expected step voltage differences (calculated) between a 3.9 V chip and a 2.6 V chip (both generating 1.5 V rms sine waves), for (a) 32 and (b) 64 samples plotted versus the sample number for one complete waveform period.

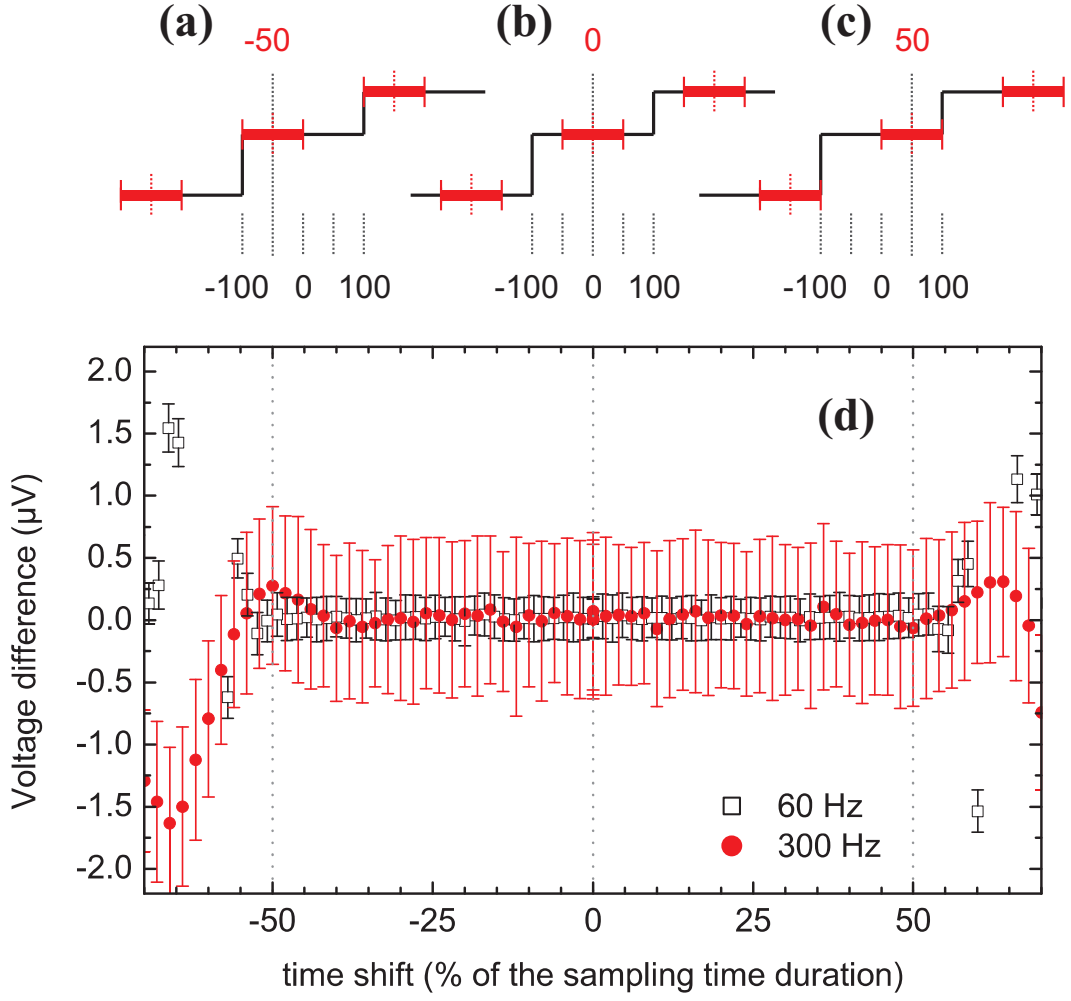


FIG. 9: (Color online) Difference between the reconstructed rms voltage and the expected ideal rms voltage for array B (2.6 V chip, 1.5 V rms) as a function of the relative time alignment with the sampling voltmeter. Array A (3.9 V chip) provides the voltage reference levels for reconstruction of the rms voltage of array B. Both plots (60 Hz and 300 Hz) use 32 samples. The upper part of the figure shows a schematic view of the sampling windows as function of the relative time shift at -50 %, 0 %, and +50 %.

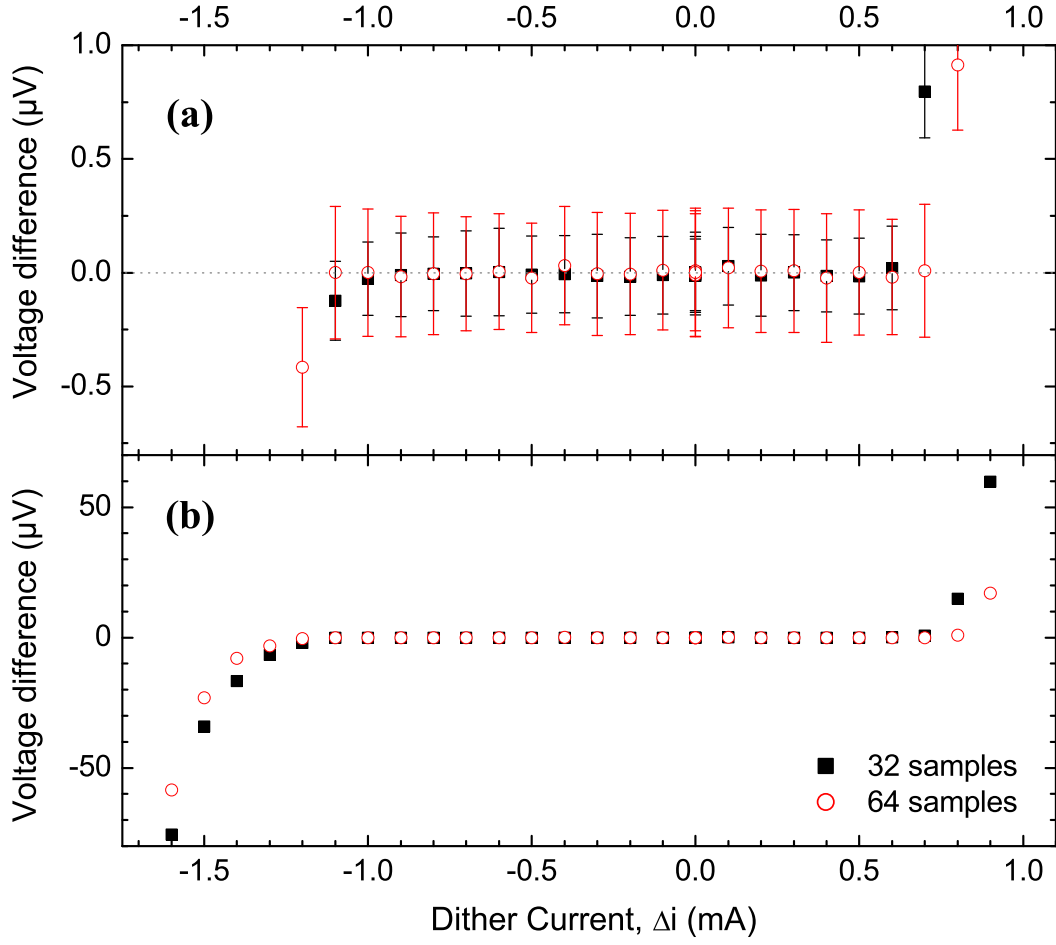


FIG. 10: (Color online) Difference between the reconstructed rms voltage and the expected ideal rms voltage for array B (2.6 V chip, 1.5 V rms) as a function of the dither current flowing in array B. Array A (3.9 V chip) provides the 1.5 V rms reference for reconstruction of the rms voltage of array B. Measurement results are shown for two different 60 Hz waveforms with 32 and 64 samples. The upper plot shows a 100 times smaller voltage range.

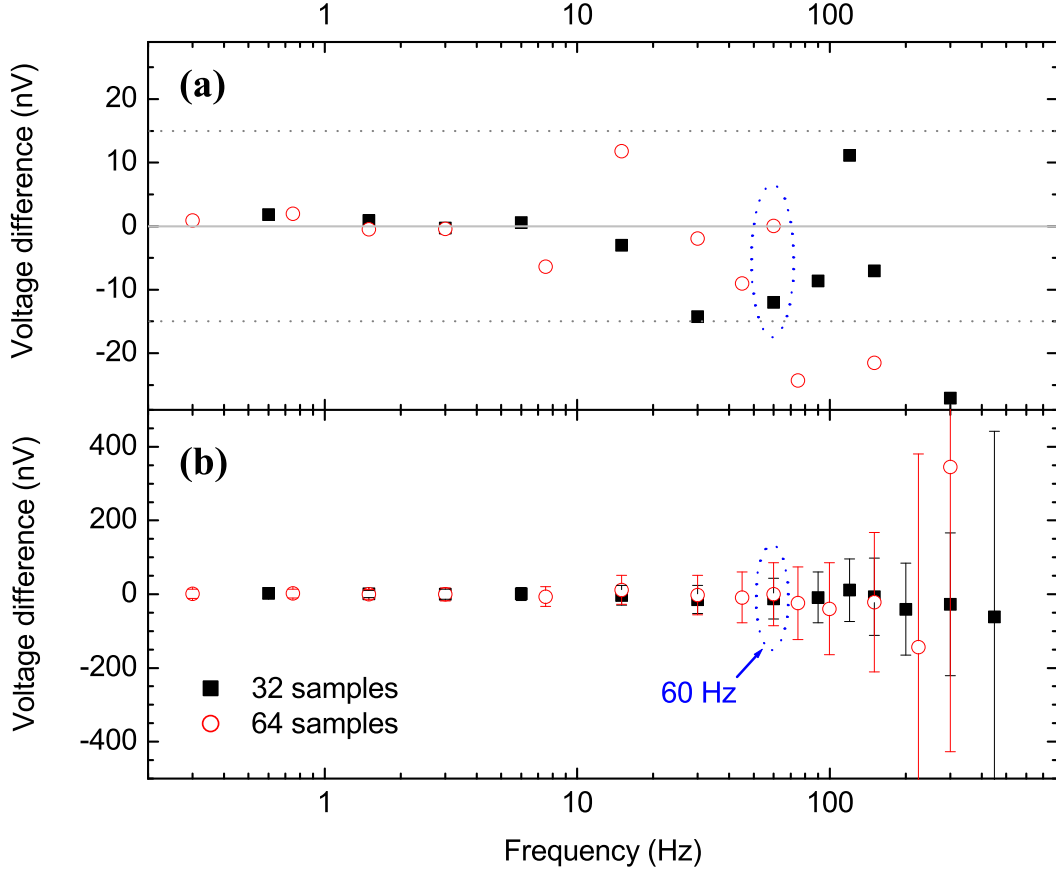


FIG. 11: (Color online) Difference between the reconstructed measured rms voltage and the expected ideal rms voltage for array B (2.6 V chip, 1.5 V rms) at different frequencies. Array A (3.9 V chip) provides the voltage reference for reconstructing the rms voltage of array B. Waveforms with both 32 and 64 samples were synthesized at each frequency. Both plots (a) and (b) show the same voltage difference, but on different voltage scales. The combined uncertainty of the measurement is only shown in (b).

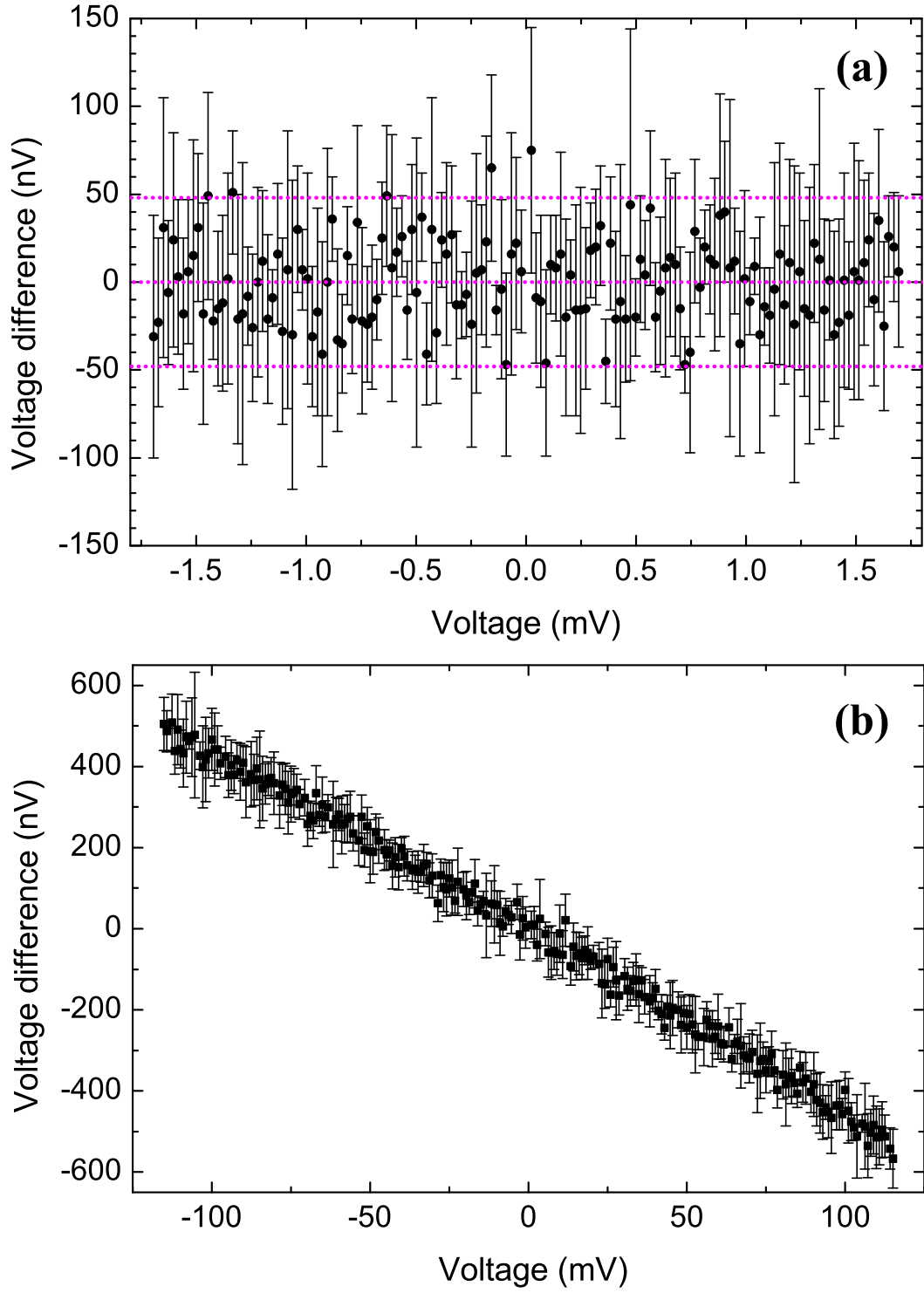


FIG. 12: (Color online) Voltmeter dc gain calibration using (a) the differential voltage generated with two arrays (1 mV), and (b) the reference voltage provided by a single array (100 mV). Both measurements are performed on the 100 mV range of the voltmeter. *Voltage difference* = *Voltage measured* - *Josephson voltage*.

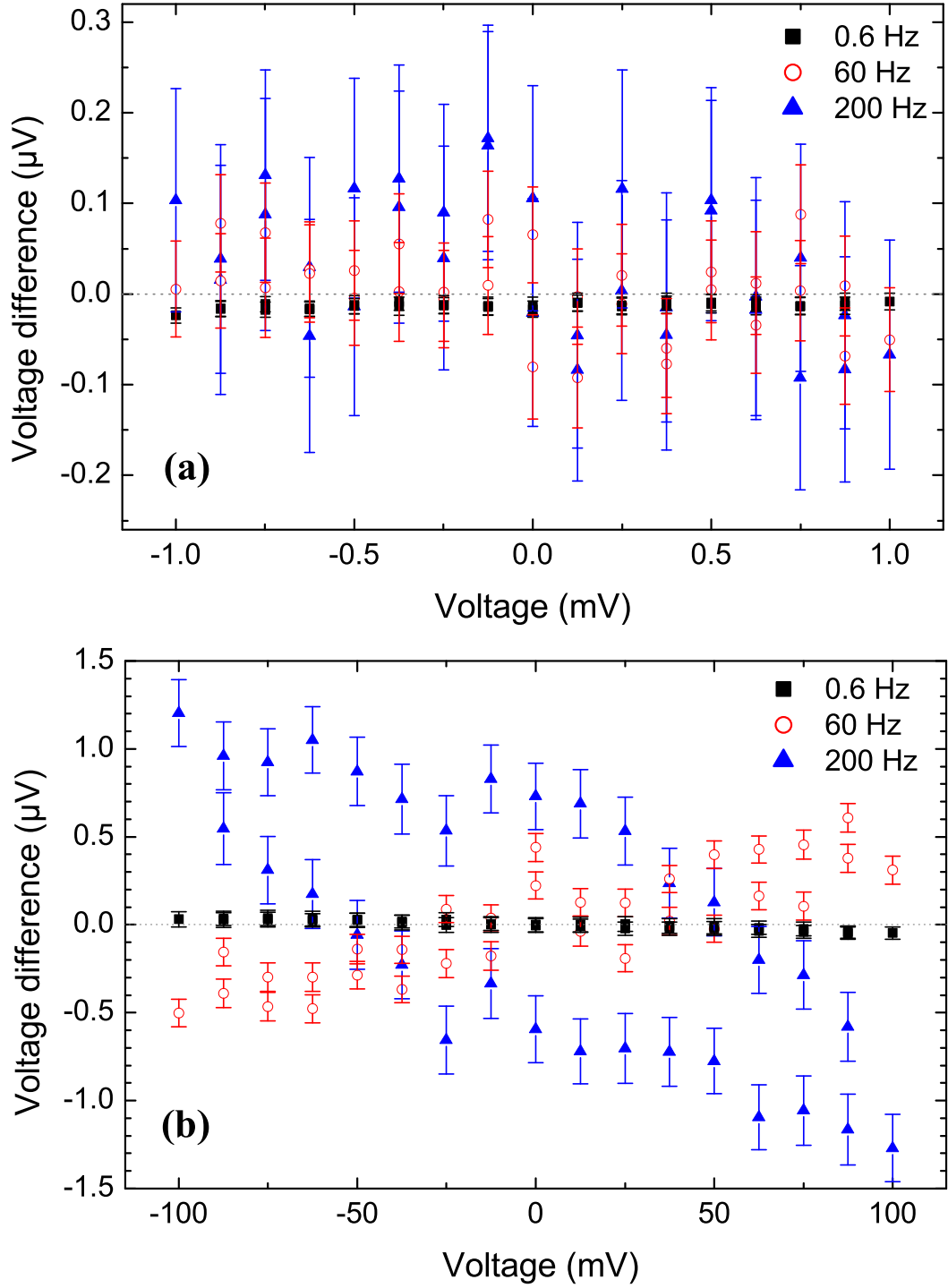


FIG. 13: (Color online) Measured gain and linearity in the sampling mode (100 mV range) using 32 sample triangular waveforms with (a) 1 mV and (b) 100 mV amplitudes. (a) The 1 mV triangle waveform is generated using the differential two-array subtraction method. (b) The 100 mV amplitude waveform is directly generated with a single system. *Voltage difference* = *Voltage measured* - *Josephson voltage*.